

Prognostic value and drug sensitivity of F-box and leucine-rich repeat protein 6 in glioma

QINGYUAN LIN^{1,2*}, JINCHAO ZHU^{1,2*}, WEIYAO ZHU^{2*}, HONGLIN ZHU¹,
MEIJUN LI², JIAQI ZHAO³, SHOUQIANG JIA⁴ and SHENGDONG NIE¹

¹School of Health Science and Engineering, University of Shanghai for Science and Technology, Shanghai 200093;

²Department of Pathology, The Ninth People's Hospital, Shanghai Jiao Tong University School of Medicine, Shanghai 200011;

³Department of Ultrasound, Shanghai Fourth People's Hospital, School of Medicine, Tongji University, Shanghai 200000;

⁴Department of Imaging, Jinan People's Hospital Affiliated to Shandong First Medical University, Jinan, Shandong 250102, P.R. China

Received December 1, 2023; Accepted March 22, 2024

DOI: 10.3892/ol.2024.14453

Abstract. Gliomas are highly malignant and invasive tumors lacking clear boundaries. Previous bioinformatics and experimental analyses have indicated that F-box and leucine-rich repeat protein 6 (FBXL6), a protein crucial for the cell cycle and tumorigenesis, is highly expressed in certain types of tumors. The high expression level of FBXL6 is reported to promote tumor growth and adversely affect patient survival. However, the molecular mechanism, prognostic value and drug sensitivity of FBXL6 in glioma remain unclear. To address this, the present study analyzed FBXL6 expression in gliomas, utilizing data from The Cancer Genome Atlas and Chinese Glioma Genome Atlas databases. Analysis of FBXL6 mRNA expression levels, combined with patient factors such as age, sex and tumor grade using Kaplan-Meier plots and nomograms, demonstrated a strong correlation between FBXL6 expression and glioma progression. Co-expression networks provided further insights into the biological function of FBXL6. Additionally, using CIBERSORT and TISDB tools, the correlation between FBXL6 expression correlation tumor-infiltrating immune cells and immune genes was demonstrated to be statistically significant. These findings were validated by examining FBXL6 mRNA and protein levels

in glioma tissues using various techniques, including western blot, reverse transcription-quantitative PCR and immunohistochemistry. These assays demonstrated the role of FBXL6 in glioma progression. Furthermore, drug sensitivity analysis demonstrated a strong correlation between FBXL6 expression and various drugs, which indicated that FBXL6 may potentially act as a future promising therapeutic target in glioma treatment. Therefore, the present study identified FBXL6 as a diagnostic and prognostic marker in patients with gliomas and highlighted its potential role in glioma progression.

Introduction

Gliomas are aggressive brain tumors that vary in incidence based on patient demographics and location, typically affecting 2-10 individuals per 100,000 in the population. Their malignant and invasive nature poses significant health challenges as high recurrence rates after radiotherapy and chemotherapy can result in high mortality rates (1,2). Although early diagnosis and surgery can improve the survival rate of patients (3), high-grade gliomas, especially glioblastomas (GBM, Grade IV), have low survival rates (4). Despite considerable treatment efforts, GBM remains the most common and aggressive form of brain tumor in humans (5). Considering that GBM is associated with high incidence, recurrence and mortality rates (6) there is a clear need for increased research efforts to identify prognostic markers and effective drugs that can improve early diagnosis and treatment.

F-box and leucine-rich repeat protein 6 (FBXL6) is a member of the leucine-rich protein family. FBXL6 serves a crucial role in phosphorylation-dependent ubiquitination, which is essential for cell development and differentiation (7). The ubiquitin-proteasome system (UPS) is an essential component of post-translational modifications and serves a critical role in various cellular activities, such as the cell cycle (8), apoptosis (9), DNA damage repair (10), immune response (11) and tumor development (12). Consequently, the study of the UPS in tumors has received increasing attention (13,14). Ubiquitination involves a three-enzyme cascade consisting of E1 (Ub-activating), E2 (Ub-conjugating) and E3 (Ub-ligase) enzymes (15). Notably, a number of F-box

Correspondence to: Professor Shouqiang Jia, Department of Imaging, Jinan People's Hospital Affiliated to Shandong First Medical University, Changdou Road West, Laiwu, Jinan, Shandong 250102, P.R. China

E-mail: jshqlw@163.com

Professor Shengdong Nie, School of Health Science and Engineering, University of Shanghai for Science and Technology, 516 Jungong Road, Yangpu, Shanghai 200093, P.R. China

E-mail: nsd4647@163.com

*Contributed equally

Key words: glioma, glioblastomas, F-box and leucine-rich repeat protein 6, prognostic marker, therapeutic target

proteins, which serve as substrate-recognition subunits within Skp1-cullin-F-box protein E3 ligase complexes, serve a crucial role in various cellular processes (16,17). Specifically, they mediate the ubiquitination and subsequent degradation of target proteins (18), primarily influencing tumor development through substrate turnover (19,20). FBXL6 activates the estrogen receptor (ER) by promoting transcription and mediating protein degradation. This highlights the significance of FBXL6 in the modulation of ER activity and the potential for targeted FBXL6-based strategies in the treatment of ER-related cancers (21). Chan *et al* (16) previously reported that FBXL6 serves a critical role in human tumor development and acts as a distinct prognostic marker for malignant progression in renal cell carcinoma (22,23). In liver cancer, the accumulation of FBXL6 promotes the stabilization and activation of c-Myc by preventing the degradation of HSP90AA1. Activated c-Myc, in turn, binds directly to the promoter region of FBXL6, inducing its mRNA expression (24). In colorectal cancer, FBXL6 is highly expressed and is associated with poor prognosis. It interacts with phospho-p53 (S315), facilitating polyubiquitination at K291/292 and consequently inhibiting the signal transduction of P53 (22). Despite these aforementioned findings, there are few reports on the impact of FBXL6 expression on gliomas and its biological function remains largely unexplored. Therefore, further investigation is necessary to determine the prognostic potential of FBXL6 and drug sensitivity in patients with glioma.

Building on previous studies, we investigated the specific role of FBXL6 in gliomas. By utilizing The Cancer Genome Atlas (TCGA), Gene Expression Profiling Interactive Analysis (GEPI) and Chinese Glioma Genome Atlas (CGGA) databases, the present study comprehensively analyzed the relationship between prognostic value, drug sensitivity and FBXL6 expression in glioma. In addition, the expression and prognostic significance of FBXL6 in gliomas was examined using various methods such as western blot, reverse transcription-quantitative PCR and immunohistochemistry (IHC). The present study may offer novel insights to guide future clinical approaches to treating human gliomas.

Materials and methods

Data and preprocessing. Gene expression data and complete clinical annotations were obtained from the CGGA (cgga.org.cn/) and TCGA (<https://portal.gdc.cancer.gov/>) databases. Patient data included the age, sex, radiotherapy and chemotherapy statuses of patients, complete follow-up information, histopathological classification and primary/recurrent status of World Health Organization (WHO) malignant gliomas. In the present study, the mRNAseq_693 and mRNAseq_325 glioma cohorts were analyzed. Tumor-immune system interactions and drug bank database (<https://www.drugbank.ca/>) analysis was used to determine the correlation between target genes and lymphocytes, immune regulators and immune checkpoints in gliomas.

Differential expression and prognostic analysis of FBXL6 in gliomas. The expression levels of FBXL6 in gliomas were analyzed using data from the TCGA database. The ‘limma’ package in the R platform was used to analyze the differential

expression of FBXL6 between normal and tumor tissues in gliomas. Low-grade gliomas typically refer to WHO grade I or II tumors, which tend to grow slowly, have distinct borders and invade surrounding tissues to a lesser extent. Patients with low-grade gliomas generally have a better prognosis (25). Conversely, high-grade gliomas usually refer to WHO grade III or IV tumors and are characterized by rapid growth, indistinct borders and high invasiveness. Patients with high-grade gliomas typically have a poorer prognosis (26). Visualization analysis was performed using the ‘ggplot2’ and ‘ggpubr’ packages in R. Additionally, the prognostic value of FBXL6 in gliomas was analyzed using the TCGA and CGGA databases.

Clinical feature correlation analysis and nomogram construction. The CGGA database provided detailed clinical data, including patient age, sex, radiotherapy and chemotherapy status, complete follow-up information, histological classification and primary/recurrent status of WHO malignant gliomas. TCGA clinical data included sex, age and tumor grade. Therefore, a detailed analysis of the correlation between FBXL6 expression and clinical features using was performed using bioinformatic tools. Receiver operating characteristic (ROC) curves were used to determine the accuracy of FBXL6 expression in predicting 1-, 3- and 5-year survival rates in patients with glioma. To construct a nomogram using both FBXL6 expression data and clinical data, the ‘rms,’ ‘survival,’ and ‘regplot’ packages in R were used to assess the impact of age, sex and tumor grade on patients with glioma. Clinical decision curve analysis was used to evaluate the accuracy of the 1-, 3- and 5-year survival rate predictions in patients with glioma. Additionally, the reliability of the nomogram was assessed using calibration curves.

Correlation between genes and enrichment analyses. To investigate the specific mechanisms underlying FBXL6 expression in gliomas, gene correlation and enrichment analyses were performed. For the correlation analysis, the filtering criteria were $R \geq 0.6$ and $P < 0.001$. To explore the biological processes and pathways related to the correlated genes in gliomas, enrichment analyses were performed using the Gene Ontology (GO), Kyoto Encyclopedia of Genes and Genomes (KEGG) pathway and Gene Set Enrichment Analysis (GSEA) databases.

Correlation between immune microenvironment, immune cell infiltration and FBXL6 expression. The role of FBXL6 expression in immune cell infiltration was investigated by using the CiberSort algorithm to study the distribution of 22 tumor-infiltrating immune cells in high and low FBXL6 expression groups. Furthermore, Spearman correlation analysis was conducted to explore the strength of the association between FBXL6 expression and the 22 types of immune-infiltrating cells. Immune and stromal scores were calculated using estimation methods to reflect the relationship between FBXL6 expression and the immune microenvironment. TIMER2 (<http://timer.cistrome.org/>) analysis FBXL6 expression in different correlation between immune cells and glioma subtypes.

Drug sensitivity analysis. With the advancement of precision medicine, the demand for personalized treatment has

increased. The sensitivity of gene expression and drugs is a critical factor in personalized treatment (27). Robust prediction of *in vivo* chemotherapy responses by collecting pretreatment baseline gene expression levels and drug sensitivity data from cancer cell lines has been a long-standing and controversial issue in pharmacogenomics. Cancer cell lines in labs may not accurately reflect patient tumor complexity, leading to possible mismatches between predicted and real responses to chemotherapy. Patient-specific genetic variations and tumor environments also affect treatment outcomes, challenging the applicability of cell line data to predict patient responses effectively. Drug response information and drug-targeting pathways were collected from the Genomics of Drug Sensitivity in Cancer database (<https://www.cancerrxgene.org/>). Spearman correlation analysis was performed to identify drugs related to the risk score.

Cell culture, western blot and RT-qPCR. The U251 cell (cat. no. TCHu 58) line was obtained from the China Center for Typical Culture Collection. LN229 (cat. no. iCell-h124) and HEB (cat. no. XY-XB-1640) cell lines were purchased from Shanghai Xuan Ya Biotechnology Co., Ltd. U251 and LN229 are high-grade glioma cell lines with overexpression of the TP53 and EGFR genes, which serve crucial roles in the pathogenesis and progression of gliomas. Additionally, U251 cells also exhibit specific gene expressions such as neurofibromin, cyclin-dependent kinase inhibitor 2A and phosphatidylinositol 3,4,5-triphosphate 3-phosphatase and dual-specificity protein phosphatase, which are associated with the pathogenesis of gliomas. HEB is a normal human brain glial cell line that exhibits a polygonal shape when adhered to the matrix, with a more uniform size and a patchy growth pattern (28). Compared to HEB cells, U251 cells have a higher apoptosis rate and a faster proliferation rate. Cells were cultured in DMEM supplemented with 10% FBS (Gibco; Thermo Fisher, Inc.), 100 units/ml penicillin and 100 mg/ml streptomycin (Gibco; Thermo Fisher, Inc.). To prepare cell samples for western blot, cells were lysed with RIPA lysis buffer (Beyotime Institute of Biotechnology). The mass of protein/lane is 150 μ g. Proteins were separated by SDS-PAGE using a XCell SureLock Mini-Cell (Invitrogen; Thermo Fisher Scientific, Inc.) and transferred to a PVDF membrane (Invitrogen; Thermo Fisher, Inc.). The concentration of the separating gel was between 6% and 8%. Membranes were blocked in 5% non-fat milk in PBS (Invitrogen; Thermo Fisher, Inc.) at room temperature for 1 h before incubation with primary antibodies overnight at 4°C. The primary antibodies used were anti-FBXL6 antibodies (cat. no. PA5-64927; 1:200; Thermo Fisher, Inc.). The membranes were then incubated with the appropriate HRP-conjugated secondary antibodies (cat. no. C510051; 1:5,000; Shanghai Sheng Gong Biology Engineering Technology Service, Ltd.) at 37°C on a shaker for 2 h. Anti-GAPDH antibodies (cat. no. b181602; 1:2,000; Abcam) were used for the reference protein. Immunoreactive bands (cat. no. WBKLS0500; Millipore Immobilon Western, ECL; EMD Millipore, Billerica, MA, USA) were quantified using ImageJ software (v.1.48; National Institutes of Health, Bethesda, MD, USA).

RNA was extracted from glioma cells using TRIzol® reagent (Invitrogen; Thermo Fisher, Inc.) and quantified using a 725 spectrophotometer (Shanghai Sunny Hengping Scientific Instrument Co., Ltd.). Oligo dT (Roche Applied Science, 10814270001) was used to prime cDNA synthesis. RT-qPCR was performed using the SYBR Green Premix Ex Taq (Takara Biotechnology Co., Ltd) on an Illumina Eco (Illumina, Inc.). Total RNA was extracted from tissue and cells using Tripure Isolation reagent (Roche Applied Science; Penzberg; Germany), according to the manufacturer's instructions. The Transcription First Strand cDNA Synthesis kit (Roche Applied Science) was used to synthesize cDNA from 1 μ g total RNA at room temperature at 24°C for 50 min. Differences in gene expression were calculated using the $2^{-\Delta\Delta Cq}$ method (29). The thermocycling conditions were as follows: Initial denaturation at 94°C for 5 min, followed by 30 cycles at 94°C for 45 sec, 59°C for 45 sec and 72°C for 45 sec, followed by 72°C for 45 sec and final extension at 72°C for 10 min. Experiments were performed in triplicate with SYBR Green I Master mix (Roche Applied Science); GAPDH was used as the internal control. The primers used were as follows: FBXL6 forward (F), 5'-CATCAACCGTAATAGCATTCCCC-3' and reverse (R), 5'-CACATCAGGTTCAACAGCCG-3' and GAPDH F, 5'-GGAGCGAGATCCCTCCAAAAT-3' and R, 5'-GGCTGTGTGTCATACTTCTCATGG-3'.

IHC. In the present study, paraffin-embedded glioma specimens and matched adjacent non-tumor tissues were surgically excised from patients at the Department of Neurosurgery and forwarded to the Department of Pathology for the pathological diagnosis of glioma. Sample collection took place from January 2020 to June 2023. Upon confirmation of glioma diagnosis, paraffin-embedded specimens were stored within the Department of Pathology. This was a retrospective study and informed consent for this study was waived because the patients had previously provided written informed consent for the use of their post-operative samples and information in future clinical research. The study protocol, including the use of these tissue samples, was approved by the Ethics Committee of the Ninth People's Hospital affiliated with Shanghai Jiao Tong University School of Medicine (approval no. H9H-2023-T489-1; Shanghai, China). Clinical samples were fixed in 4% paraformaldehyde at room temperature for 24 h, subsequently embedded in paraffin, and sectioned to a uniform thickness of 3 micrometers. Immunostaining was performed using the two-step Elivision Plus kit system (Dako; Agilent Technologies, Inc.). The sections were dewaxed in xylene, rehydrated with a series of ethanol solutions (100, 95, 80 and 70%), and then boiled in ethylenediaminetetraacetic acid buffer (pH 9.0) for 20 min in an autoclave. Next, 0.3% H₂O₂ was used to block endogenous peroxidase activity at room temperature for 15 min, and the sections were incubated with normal goat serum (1:20; Beyotime Institute of Biotechnology) for 20 min at room temperature to reduce non-specific binding. Tissue sections were incubated with the anti-FBXL6 (cat. no. PA5-64927; 1:200; Thermo Fisher) for 50 min at room temperature. The secondary antibody was applied using the Envision Detection kit (SM802; Dako; Agilent Technologies; Ready-to-use type) for 20 min at room temperature. Slides were stained for 2 min with diaminobenzidine tetrahydrochloride

(DAB) and then counterstained 2 min with hematoxylin at room temperature. The completed sections were mounted using a neutral resin (K-0212, Shanghai Jiehao Biotechnology Co., Ltd.). The stained tumor cells were assessed with a Nikon conventional optical microscope in 10 independent fields at magnification, x400. Immunohistochemical image results were quantified using ImageJ software (v.1.48; National Institutes of Health, Bethesda, MD, USA). All the sections were scored by two independent pathologists who were blinded to the type of sample. Specifically, the intensity of positive cytoplasmic staining was rated on a scale of 0-3 (0, negative; 1, light brown; 2, medium brown; and 3, dark brown). The corresponding percentages of positively stained cells were set as: 1, 1-25%; 2, 26-50%; 3, 51-75%; and 4, 76-100%.

Statistical analysis. All statistical analyses were performed using R (version 4.1.2; RStudio, Inc.). The results are presented as the median \pm interquartile range or mean \pm standard deviation (SD). Western blot data were analyzed using GraphPad Prism (version 5; Dotmatics). One way ANOVA was employed to compare the means \pm SD between two groups followed by the Least Significant Difference posts hoc test. The Chi-square test and Fisher's exact test were utilized for analyzing qualitative data. For comparisons between two groups, the Mann-Whitney U test (non-parametric) was used, while the Kruskal-Wallis test followed by Dunn's test was applied for comparisons involving >2 groups. The log-rank test and Kaplan-Meier survival analysis were used to compare prognosis among the different risk groups. Univariate and multivariate Cox regression analyses were performed to evaluate the prognostic value of risk models. The significance of the correlation was assessed using the Spearman's rank correlation test. All experiments were validated with three repeated trials. $P < 0.05$ was considered to indicate a statistically significant difference.

Results

High FBXL6 expression was associated with poor prognosis in glioma. The data collection and analysis performed in the present study (Fig. 1) identified key biomarkers in glioma. Multicenter screening and validation were performed and FBXL6 was identified as a key marker. Compared with normal tissues, pan-cancer analysis demonstrated that FBXL6 was highly expressed not only in GBM, but also in certain other cancers, including bladder, breast and colorectal cancers (Fig. 2A). TCGA-glioma analysis demonstrated consistently higher FBXL6 expression in tumor tissues compared with normal tissues in the TIME2 database (Fig. 2B). Kaplan-Meier curve analysis of TCGA-glioma data demonstrated that high FBXL6 expression was associated with decreased overall survival and progression-free survival compared with low FBXL6 expression, an unfavorable outcome for patients with glioma (Fig. 2C-D). Moreover, the CGGA database showed the same relationship between FBXL6 expression and prognosis (Fig. 2E). Western blot was performed to examine the FBXL6 protein levels in glioma U251 and normal HEB cells. The protein expression level of FBXL6 was higher in U251 cells compared with HEB cells (Fig. 3A). The RT-qPCR results demonstrated that FBXL6 mRNA expression levels

were significantly higher in U251 compared with HEB cells (Fig. 3B). Given the crucial role of FBXL6 in cancer (22,30), its expression levels were investigated across different stages of glioma. A tissue microarray comprising samples from 64 glioma patients was constructed for this purpose. Patients were stratified into two groups based on their IHC Score (IRS): i) Low-expression group, $IRS \leq 7$; ii) and High-expression group, $IRS \geq 8$. Subsequently, the expression level of FBXL6 in the glioma tissue microarray was assessed via IHC. Compared with low-grade glioma, the expression of FBXL6 protein increases in high-grade gliomas. Furthermore, the protein expression level of FBXL6 was increased in patients with glioma at WHO Grade IV compared with patients at WHO Grade II stage (Fig. 3C,D; Table I). These findings suggested that the high expression of FBXL6 in glioma may affect its biological function.

FBXL6 expression correlated with clinical features of glioma. CGGA, univariate (Fig. 4A) and multivariate (Fig. 4B) COX regression analyses demonstrated that FBXL6 expression was associated with poor survival and was considered an independent prognostic factor in each dataset. FBXL6 was also associated with IDH mutations, Primary, Recurrent and Secondary status, WHO grade, chemotherapy regime and 1p19q co-deletion. Therefore, FBXL6 may have a high predictive value in patients with gliomas and could potentially be used as a prognostic factor for gliomas. In addition, the expression level of FBXL6 was significantly higher in patients with glioma undergoing chemotherapy compared with those not undergoing chemotherapy (Fig. 4C). According to the WHO classification, the higher the glioma grade, the higher the expression level of FBXL6 (Fig. 4D). In various subtypes of pathological tissues, the expression of FBXL6 was correlated with multiple subtypes of glioma and compared with other subtypes, FBXL6 had the highest expression level in glioblastoma (Fig. 4E). There was no statistical significance observed between FBXL6 expression levels and the IDH1 mutation or 1p19q codeletion status (Fig. S1A-B). These results suggested that FBXL6 expression promoted the occurrence and development of glioblastoma and could potentially serve as a potential molecular marker.

ROC curve prediction and nomogram construction for glioma prognosis. Given the significant correlation between FBXL6 expression and clinical factors such as tumor grade and age (Fig. 5A), the survival rates of patients with glioblastoma over 1-, 3- and 5-year periods were predicted using FBXL6 expression levels. The ROC curve demonstrated that FBXL6 expression was strongly predictive of the survival rates of patients with glioblastoma, with AUC values of 0.573, 0.639 and 0.631 for the 1-, 3- and 5-year survival rates, respectively (Fig. 5B). A nomogram was constructed to predict the correlation between FBXL6 expression and age, sex and tumor grade, which demonstrated a significant clinical predictive value for FBXL6 expression according to age and grade. Confidence in the validity of the nomogram was further reinforced by clinical calibration curve data (Fig. 5C,D).

Genetic correlations, biological functions and GSEA enrichment analysis of FBXL6 in glioma. To explore the specific

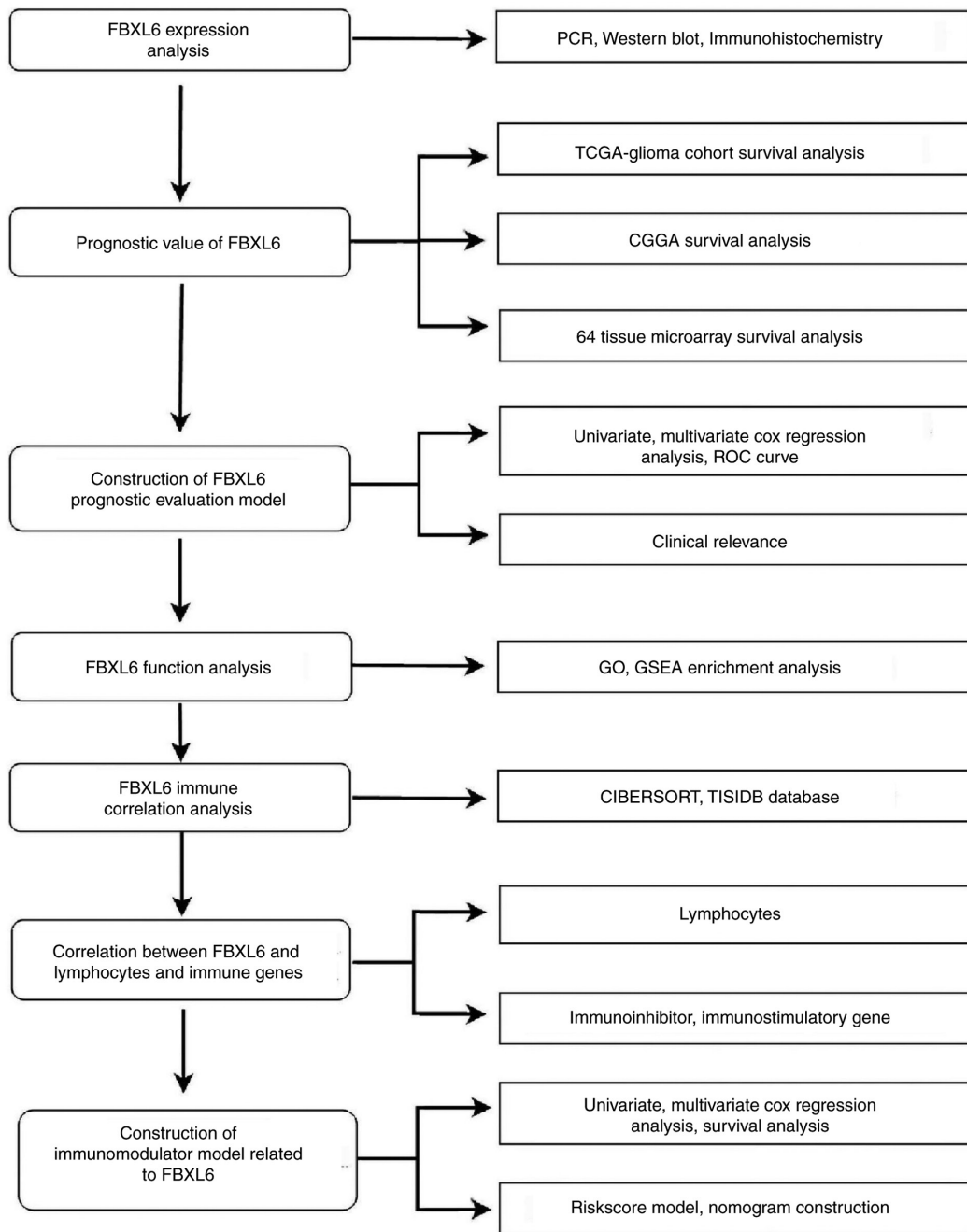


Figure 1. Data collection and analysis flow chart for FBXL6 expression in glioma. FBXL6, F-box and leucine-rich repeat protein 6; TCGA, The Cancer Genome Atlas, CGGA, Chinese Glioma Genome Atlas; ROC, receiver operating characteristic; GO, Gene Ontology; GSEA, gene set enrichment analysis; TISIDB, tumor-immune system interactions and drug bank database.

biological functions of FBXL6 in glioblastoma, gene correlation analysis was performed with a correlation threshold of 0.6 and $P < 0.001$. The results demonstrated that FBXL6 expression was positively correlated with mitochondrial RHO GTPase 2, aarF domain-containing protein kinase 5, uridine-cytidine kinase-like 1, AP-4 complex accessory subunit Tepsin, zinc finger protein GLI4 and signal peptide peptidase-like 2B and significantly negatively correlated with solute carrier family 2, facilitated glucose transporter member 12, growth hormone-inducible transmembrane protein, phosphatidylethanolamine-binding protein 4 and TLC domain-containing protein 4 (Fig. 6A). The general control of nucleotide synthesis 5 (GCN5) is an enzyme that serves a critical role in

the modification of histones, influencing gene expression by adding acetyl groups to the histone proteins, which impacts the structure and function of chromatin. Gene correlation analysis demonstrated a significant correlation between FBXL6 and GCN5, which was consistent with previous research (Fig. S2). Furthermore, the expression of FBXL6 was positively correlated with IDH1 and negatively correlated with MGMT. However, the expression of GCN5 demonstrated no significant correlation with IDH1 and was negatively correlated with MGMT (Fig. S3). Gene Expression Profiling Interactive Analysis 2 database (gepia2.cancer-pku.cn/#/index) investigates the relationship between the expression of FBXL6 and GCN5 and their correlation with isocitrate dehydrogenase 1

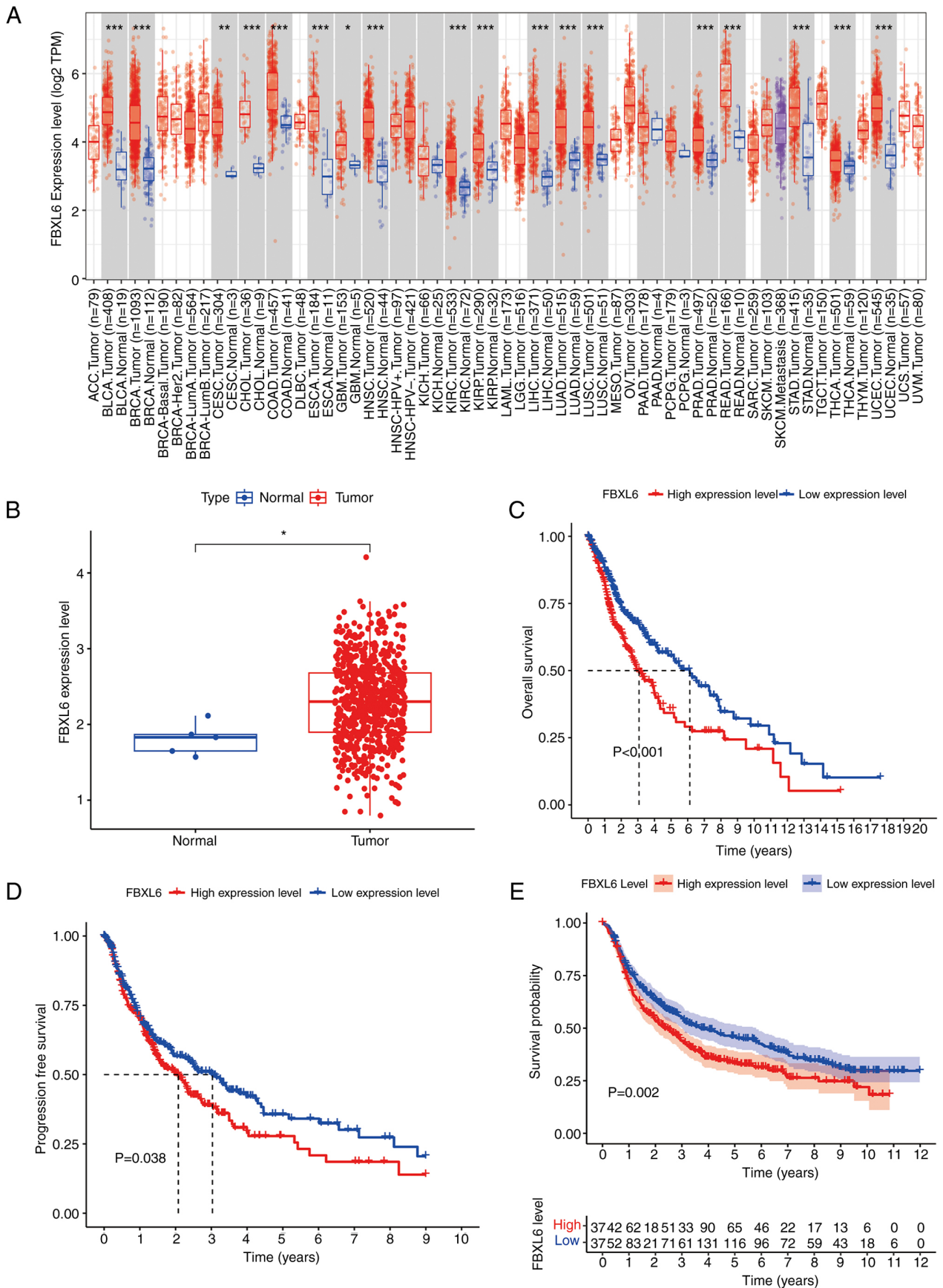


Figure 2. FBXL6 expression profile in CGGA dataset. (A) Pan-cancer expression of FBXL6. (B) Higher FBXL6 expression was observed in glioma tumors compared with normal tissues. (C) Lower overall survival was observed in patients with glioma with high FBXL6 expression levels compared with low FBXL6 expression levels. (D) Lower progression-free survival was demonstrated in patients with glioma with high FBXL6 expression levels compared with low FBXL6 expression levels. (E) Reduced overall survival in Chinese Glioma Genome Atlas database patients with glioma with high FBXL6 expression levels compared with low FBXL6 expression levels. Data were presented as median ± interquartile range and analyzed using the Mann-Whitney U test. *P<0.05, **P<0.01, ***P<0.001. FBXL6, F-box and leucine-rich repeat protein 6.

Table I. Tissue microarray clinical features from 64 patient samples.

Clinicopathological feature	Total patients, n (%)	FBXL6 expression level		P-value
		Low, n (%)	High, n (%)	
Number of patients, n	64	33	31	
Sex				0.825
Male	36 (56.3%)	19 (57.6%)	17 (54.8%)	
Female	28 (43.7%)	14 (42.4%)	14 (45.2%)	
Age, years				<0.01
≥45	38 (59.4%)	13 (39.4%)	25 (80.6%)	
<45	26 (40.6%)	20 (60.6%)	6 (19.6%)	
Grade				
I	3 (4.7%)	3 (9.1%)	0 (0.0%)	0.2388
II	24 (37.5%)	19 (57.6%)	5 (16.1%)	0.0008
III	17 (26.6%)	6 (18.2%)	11 (35.5%)	0.1594
IV	20 (31.2%)	5 (15.1%)	15 (48.4%)	0.0065

χ -square test and Fisher's exact test were used for statistical analysis.

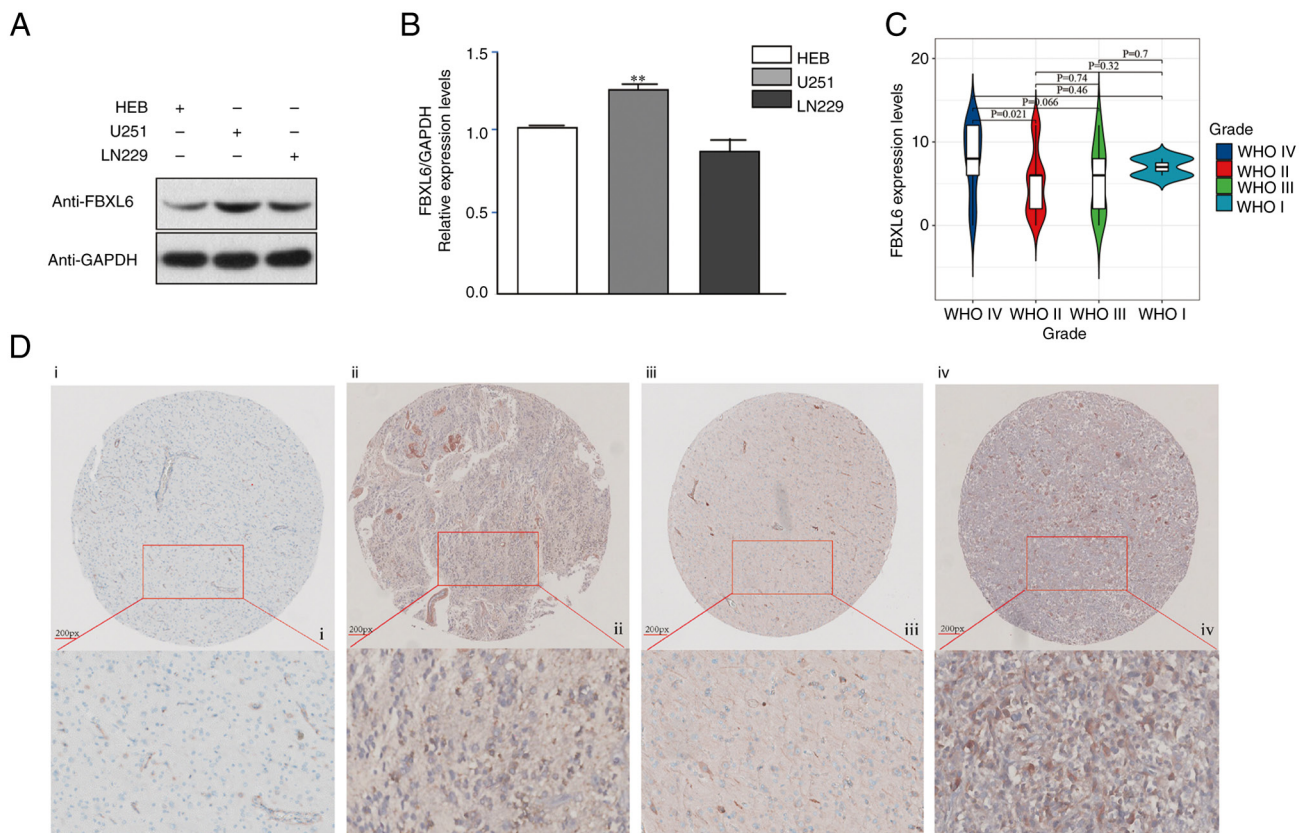


Figure 3. FBXL6 expression in human glioma cells. (A) Protein expression levels of FBXL6, with an approximate molecular weight of ~65 kDa, analyzed by western blot. (B) mRNA expression levels of FBXL6 analyzed by reverse transcriptase-quantitative PCR. Data were presented as mean \pm standard deviation and were analyzed using ANOVA followed by the Least Significant Difference post hoc test. (C) Schematic representation of the IHC expression of FBXL6 in gliomas from Grades I-IV. Data were presented as the median \pm interquartile range and were analyzed using the Kruskal-Wallis test followed by Dunn's post hoc test. (D) FBXL6 expression in patients with glioma from WHO grades II-IV analyzed using IHC. ** $P < 0.01$. FBXL6, F-box and leucine-rich repeat protein 6; WHO, World Health Organization; IHC, immunohistochemistry.

(IDH1) and methylated DNA-protein-cysteine methyltransferase (MGMT). These findings indicated that FBXL6 and

these correlated genes may influence the progression of glioblastoma.

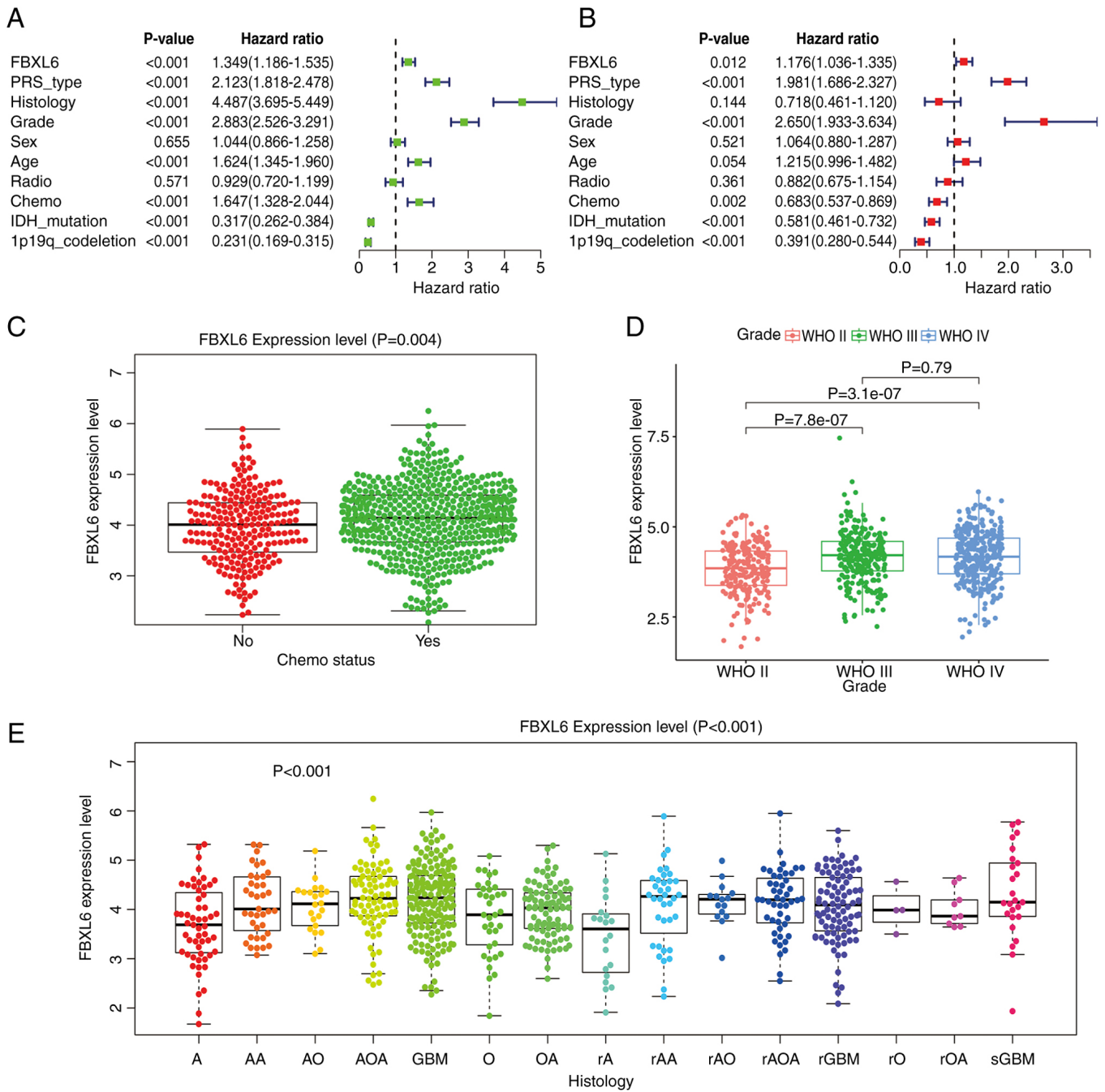


Figure 4. Association between FBXL6 expression levels and clinical traits in the Chinese Glioma Genome Atlas database. (A) Univariate and (B) multivariate analysis demonstrating a significant association between tumor grade, recurrence, IDH mutation and 1p19q co-deletion. (C) Higher FBXL6 expression levels were demonstrated in patients who received chemotherapy compared with patients who did not receive chemotherapy. (D) Higher FBXL6 expression levels were demonstrated in patients with WHO Grade IV compared with grades III and II. (E) Higher FBXL6 expression levels were demonstrated in GBM compared with low-grade gliomas. Data were presented as the median \pm interquartile range and analyzed using the Kruskal-Wallis test followed by Dunn's post hoc test. GBM, glioblastoma; FBXL6, F-box and leucine-rich repeat protein 6; WHO, World Health Organization; IDH, isocitrate dehydrogenase; radio, radiotherapy; chemo, chemotherapy; PRS, Polygenic Risk Score; GBM, glioblastoma.

Gene correlation analysis identified FBXL6 as positively associated with SPPL2B, GLI4, and ADCK5, and negatively with TLCD4, PEBP4, and GHITM (Fig. 6A,B). The GO analysis revealed significant connections to biological processes like 'organelle image', 'nuclear division', and 'chromosome aggregation', underscoring FBXL6's involvement in key cellular activities and structures. In terms of molecular function, FBXL6 expression was associated with 'channel activity', 'passive transmembrane transport' and 'transporter activity'

(Fig. 6C). GSEA enrichment analysis demonstrated that the calcium signaling pathway, cell adhesion molecule cascades and long-term potentiation were differentially enriched in patients with high FBXL6 expression (Fig. 6D).

FBXL6 expression and its impact on immune cell infiltration in glioma. FBXL6 expression was correlated with immunomodulators in gliomas including lymphocytes, immunoinhibitory and immunostimulatory molecules and

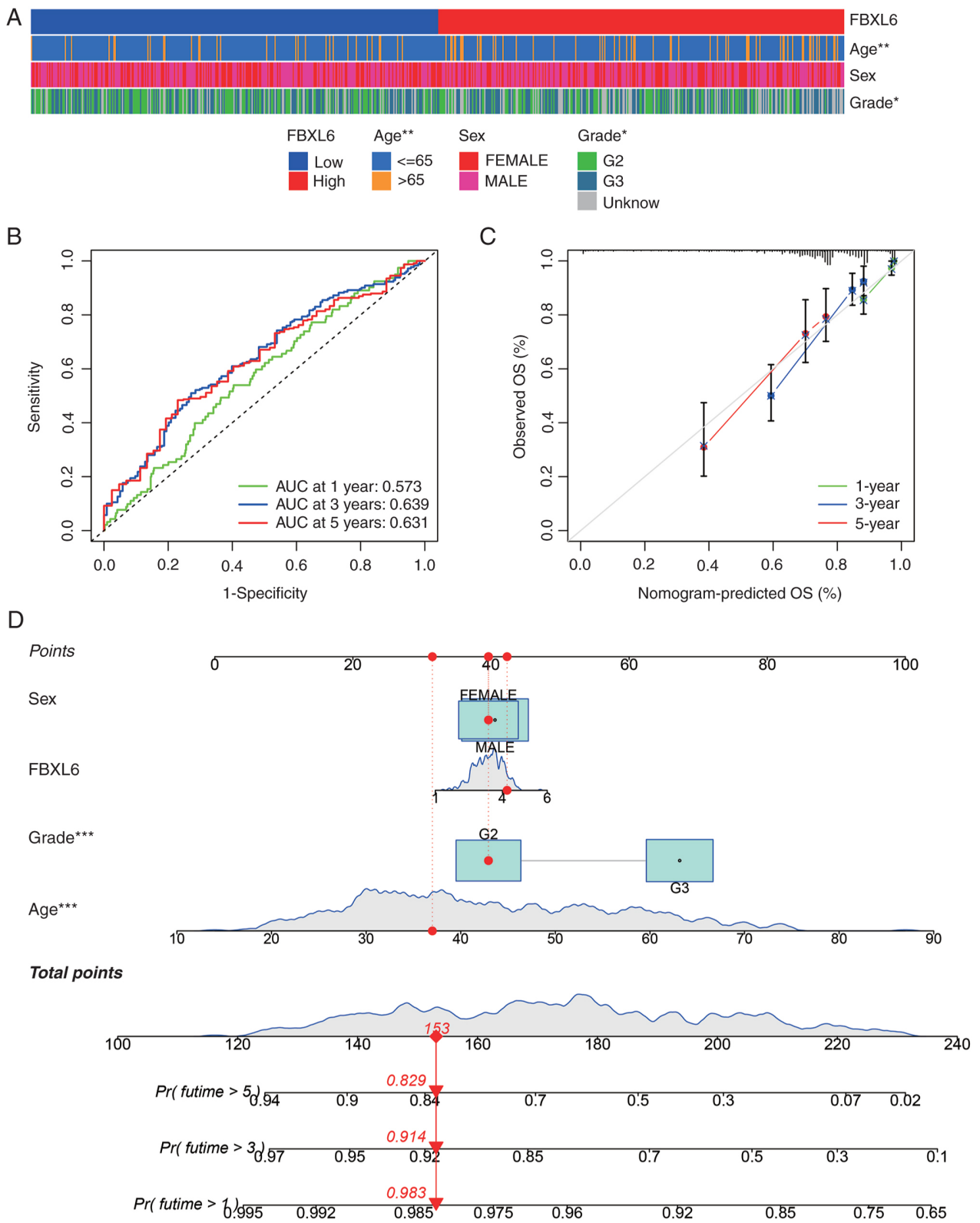


Figure 5. Clinical phenotypes and nomogram prediction based on FBXL6. (A) Heatmap of FBXL6 expression and clinical feature correlation in The Cancer Genome Atlas glioma data. (B) Receiver Operating Characteristic curve for 1-, 3- and 5-year survival rate predictions in patients with glioblastoma. (C) Calibration curves for 1-, 3- and 5-year survival rate predictions. (D) Nomogram integrating sex, age and grading. *P<0.05, **P<0.01, ***P<0.001. FBXL6, F-box and leucine-rich repeat protein 6; OS, overall survival; AUC, area under the curve; G, grade; Pr, Probability; Futime, follow-up time.

major histocompatibility complex (MHC) molecules. The association between FBXL6 expression and the expression of immunomodulatory genes in gliomas was also examined. In lymphocytes, FBXL6 expression was positively correlated with

CD56dim, whereas it showed significant negative correlations with effector memory CD4T cells and interstitial dendritic cells (Fig. 7A). Furthermore, FBXL6 expression was significantly positively correlated with the expression of immune-inhibiting

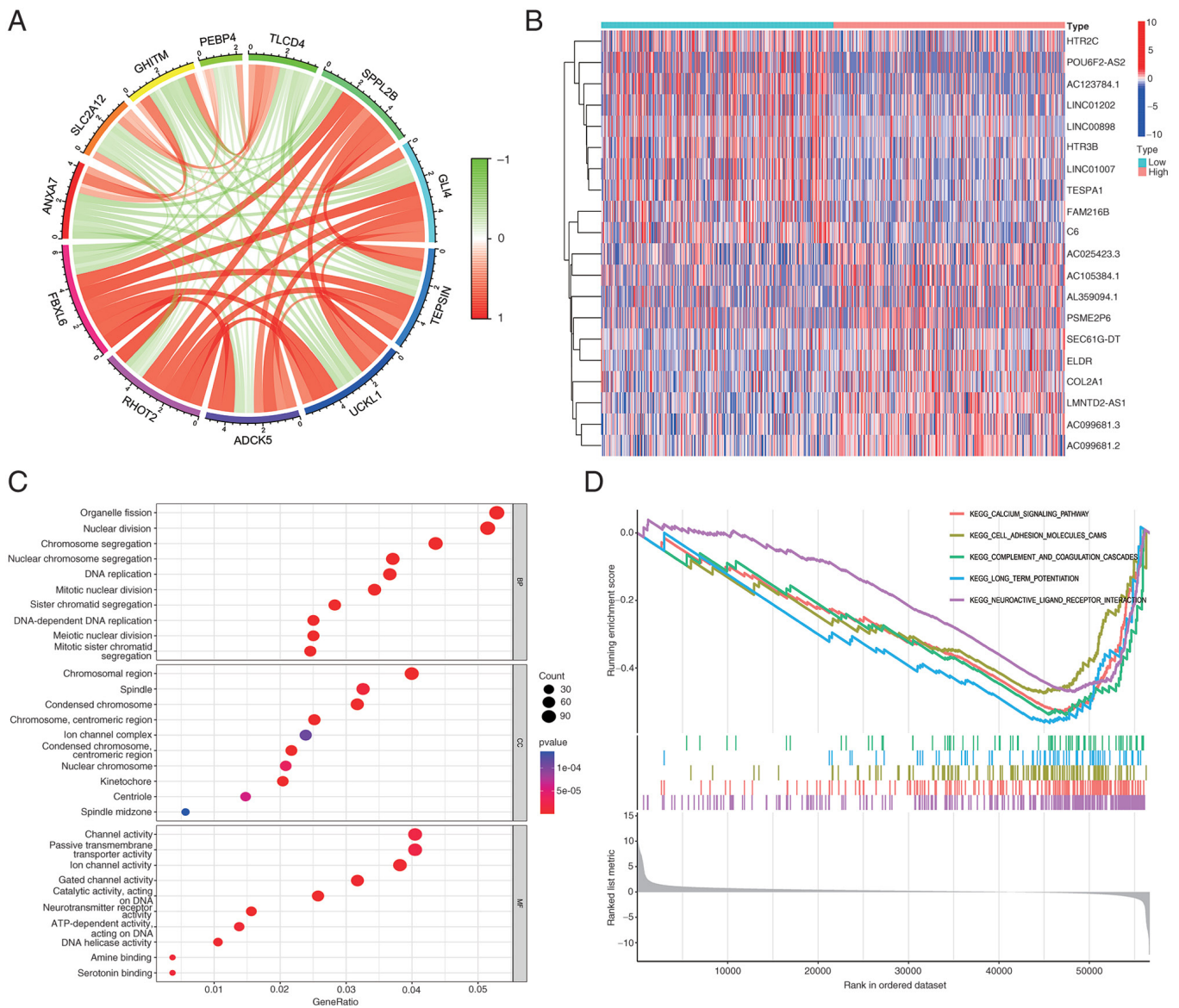


Figure 6. Biological function and GSEA of FBXL6 expression. (A,B) Correlation gene analysis. (C) Gene Ontology enrichment analysis. (D) GSEA. GSEA, Gene Set Enrichment Analysis; FBXL6, F-box and leucine-rich repeat protein 6.

genes, adenosine receptor 2a and lymphocyte activation gene 3 protein, whereas it was negatively correlated with TGF- β receptor 1 expression (Fig. 7B). Considering immunostimulatory factors, FBXL6 expression in glioblastomas demonstrated a positive correlation with tumor Necrosis Factor Receptor Superfamily Member 25), whereas it showed a negative correlation with IL-6 receptor expression (Fig. 7C). However, for MHC molecules, the expression of FBXL6 demonstrates a significant positive correlation with TAPBP (TAP Binding Protein; Fig. 7D). The analysis of the TIMER2 database indicated that in GBM and low-grade glioma subtypes, the expression of FBXL6 was negatively correlated with CD8 T cells and positively correlated with B cells (Fig. S4). These results suggested that FBXL6 may contribute to the malignant progression of glioblastoma through its multifaceted involvement in the tumor immune interaction system.

In addition, the relevance of FBXL6 expression in the tumor immune microenvironment was assessed by estimating the stromal and immune scores of the high- and low-expression

groups. Low expression of FBXL6 was significantly associated with lower stromal and immune cores (Fig. 8A), which may contribute to tumor immune escape and suppression, thereby promoting glioblastoma progression (30). Similarly, in immune-infiltrating cells, low expression of FBXL6 was significantly correlated with CD4+ memory cells and monocytes, which was consistent with our previous results and may contribute to immune evasion and promote malignant progression in patients with glioblastoma (30). Additionally, a high expression level of FBXL6 was significantly associated with M0 macrophages (Fig. 8B), whereas FBXL6 expression predominantly correlated with memory resting CD4 T cells, memory activated CD4 T cells and monocytes (Fig. 8B). The association between immune cells and FBXL6 expression using CIBERSORT was further explored and it was demonstrated that M2 and M0 macrophages were significantly positively correlated with FBXL6 expression and significantly negatively correlated with monocytes and memory resting CD4 T cells (Fig. 8C-F).

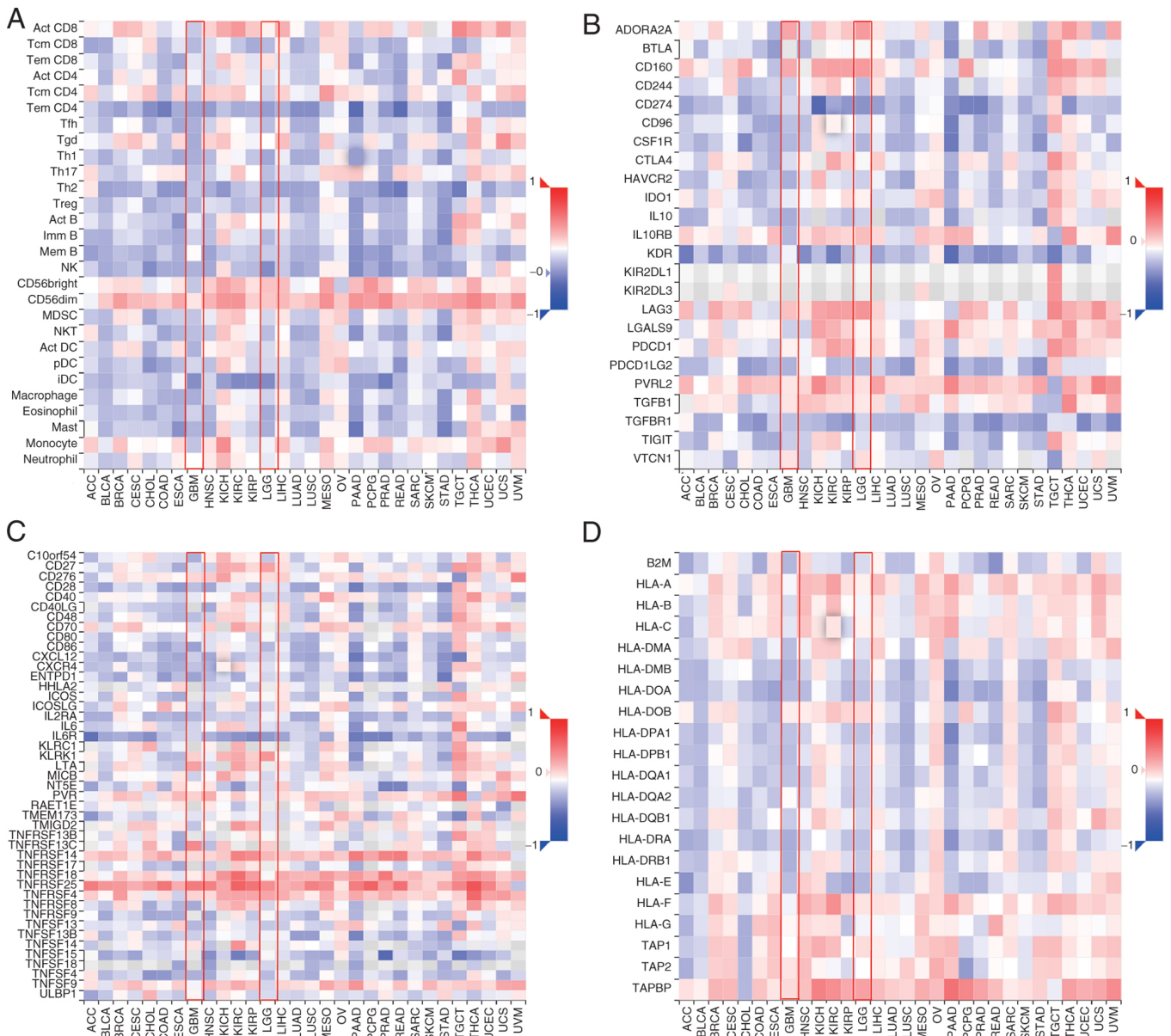


Figure 7. Correlation heatmap between F-box and leucine-rich repeat protein 6 expression levels and tumor-immune system interactions and drug bank database data. Correlation with (A) lymphocytes, (B) immunoinhibitory molecules, (C) immunostimulatory molecules and (D) Major histocompatibility complex molecules. Red color represents a positive correlation whereas blue color represents negative correlation.

Analyzing the relationship between FBXL6 expression and drug sensitivity in glioma. With the continued advancement of precision medicine and increasing demand for personalized treatment, the relationship between FBXL6 expression and the IC₅₀ of certain drugs in glioma treatments was investigated to elucidate their possible application in the individualized treatment of glioma. The R package ‘oncoPredict’ was used to predict the relationship between FBXL6 expression and drugs with a screening condition of P<0.001. Statistically significant differences in the sensitivity of eight anti-cancer drugs between the high and low groups of FBXL6 expression were found. A total of nine of these drugs (BMS345541, gefitinib, axitinib, bexarotene, foretinib, BHG712, BX-795, BX-912 and phenformin) had a higher IC₅₀ in the low FBXL6 expression group compared with the high FBXL6 expression group, which demonstrated that the patients with high levels

of FBXL6 expression may be more sensitive to treatment with these particular anticancer drugs (Fig. 9). These results suggested that these drugs may serve a potential role in the future treatment of gliomas with high FBXL6 expression.

Discussion

Glioblastoma is the most common type of brain tumor with a relatively high mortality rate due to its high recurrence rate and the difficulties associated with complete surgical resection. Although the conventional treatment method for glioblastoma involves a combination of surgery, radiotherapy and chemotherapy, this approach has not resulted in substantial improvements in patient survival rates (31). According to the WHO, the typical survival period for Grade IV malignant glioma is <20 months after diagnosis (32). The 5-year

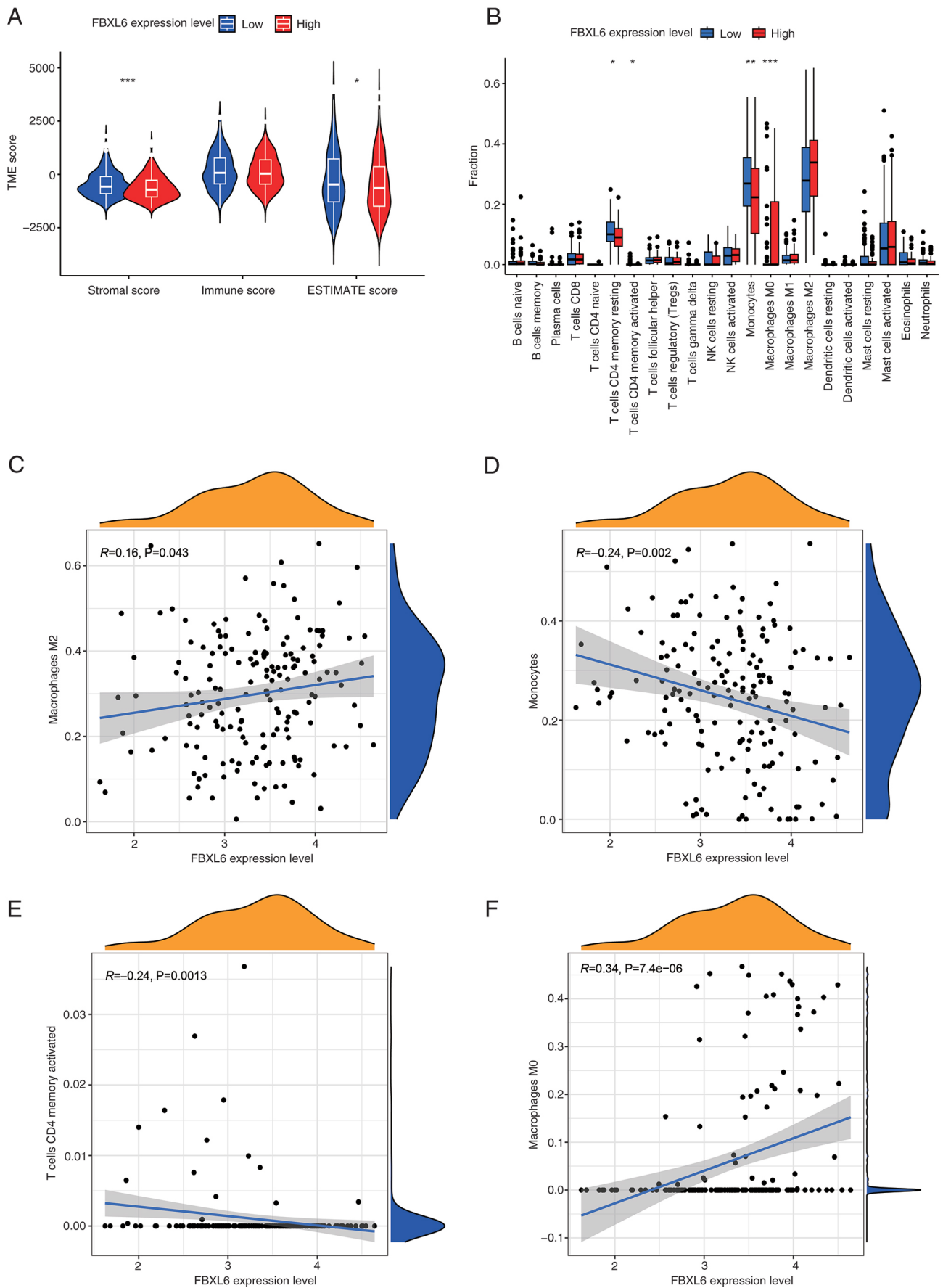


Figure 8. FBXL6 expression levels and its prognostic significance in TMB. (A) Relevance to tumor immune microenvironment. (B) Relationship with immune infiltrating cells. (C) FBXL6 expression level was positively correlated with M2 macrophages ($P=0.043$). (D) FBXL6 expression level was negatively correlated with monocytes ($P=0.002$). (E) FBXL6 expression level was negatively correlated with memory resting CD4 T cells ($P=0.0013$). (F) FBXL6 expression level was positively correlated with M0 macrophages ($P<0.001$). Data were presented as the median \pm interquartile range and analyzed using the Mann-Whitney U test. * $P<0.05$, ** $P<0.01$, *** $P<0.001$. TMB, Tumor Mutational Burden; FBXL6, F-box and leucine-rich repeat protein 6; TME, tumor immune microenvironment.

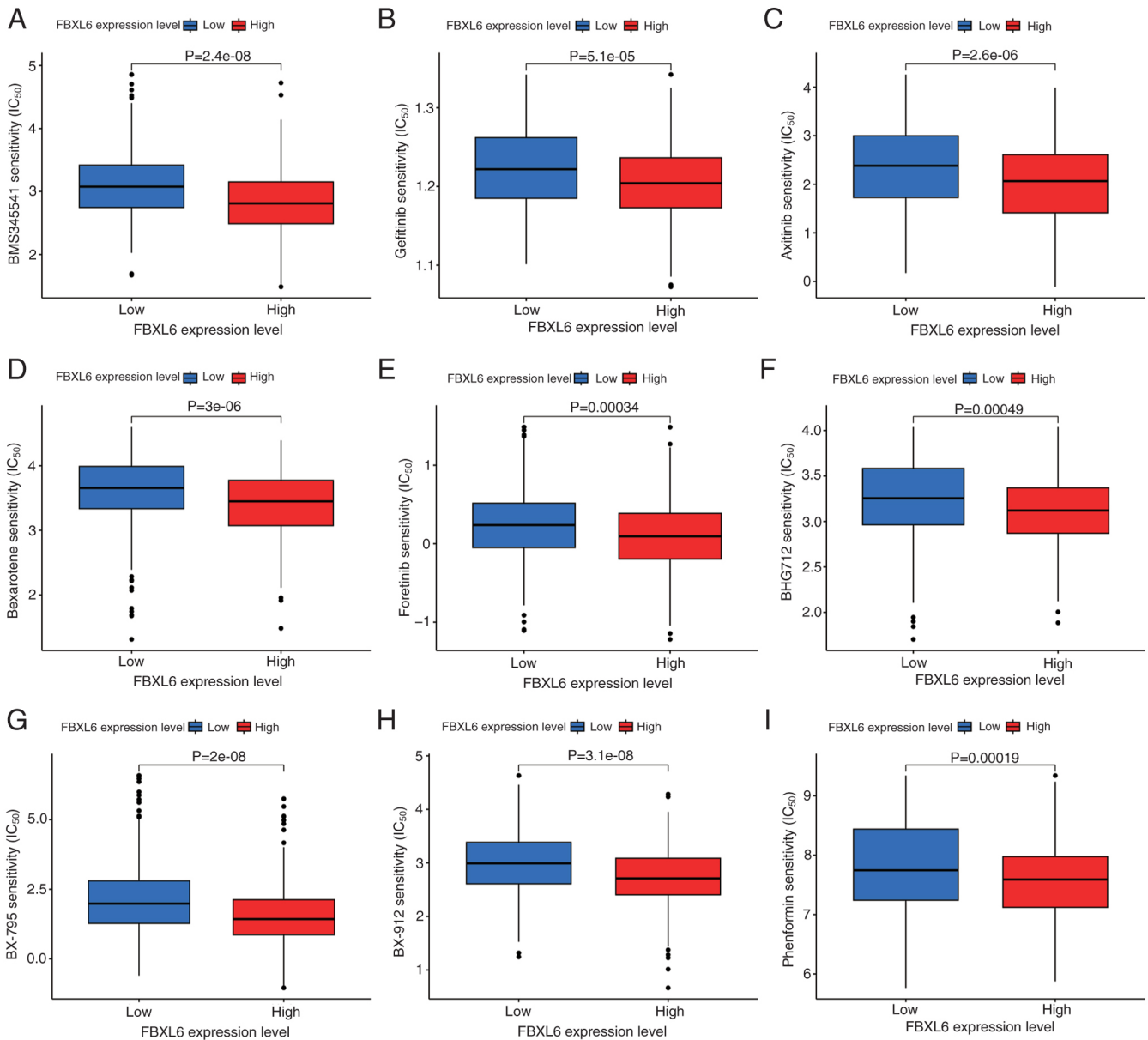


Figure 9. Drug sensitivity analysis for potential FBXL6-targeted treatments. FBXL6 has been identified as being more responsive to drugs such as (A) BMS345541, (B) Gefitinib, (C) Axitinib, (D) Bexarotene, (E) Foretinib, (F) BHG712, (G) BX-795, (H) BX-912 and (I) Phenformin in the high-risk group. Data were presented as the median \pm interquartile range and analyzed using the Mann-Whitney U test. FBXL6, F-box and leucine-rich repeat protein 6.

survival rate for patients with glioblastoma is $<5\%$ and it is lower for elderly patients aged over 65 years old. (33). Whilst Liu *et al* (34) previously reported progress with bevacizumab in improving the survival of patients with glioma, its effectiveness remains unclear. Early detection and treatment can significantly improve the prognosis of patients with gliomas (35). Therefore, it is crucial to identify new biomarkers for the early diagnosis of gliomas.

Ubiquitination serves a crucial role as an important component of various biological processes such as the cell cycle, apoptosis and DNA damage repair. The impact of ubiquitination on tumors has previously been reported (14). An enzyme that mediates ubiquitination is the E3 ubiquitin ligase, which determines the specificity of substrate ubiquitination and degradation (36). Dysregulation of F-box protein-mediated protein degradation has been implicated

in the development of human malignancies. F-box proteins can be divided into three subfamilies based on the presence of specific substrate recognition domains (37). The Fbxw subfamily consists of 10 proteins, including β -TrCP1, Fbxw7 (also known as Fbw7 and Cdc4), and β -TrCP2 (Fbxw11) (18). Owing to the close association of F-box family members with tumorigenesis, previous studies have reported certain biological functions attributed to several initially uncharacterized domains of FBXO proteins (38-41). For example, FBXO6 binds to glycosylated degradation proteins on the alpha chain of T cell receptors (42), whereas FBXO2 can ubiquitinate proteins with N-linked high-mannose oligosaccharides, such as the precursor form of β 1 integrin (43). F-box proteins serve important roles in tumorigenesis by regulating substrate turnover. Substrate turnover can be dependent or independent of E3 ligase activity (19,20). In particular, several

F-box proteins have emerged as potential therapeutic targets for cancer treatment because their dysregulation is associated with tumorigenesis (18). Emerging experimental and clinical data suggest aberrations in cell cycle regulatory factors, many of which have tumor-suppressive or oncogenic functions (44). Based on the crucial role of F-box proteins in cell cycle regulation, the key role of F-box proteins in tumorigenesis has been reported (45). In a study involving FBXL7 knockout mice, severe and progressive hematopoietic failure was observed by 12 weeks of age, with the development of T-cell acute lymphoblastic leukemia within 16 weeks (46). In tumor multi-omics research, a large number of genes associated with tumor prognosis have been discovered through bioinformatics (47). However, the effect of FBXL6 on gliomas remains unclear and requires further investigation. The present study demonstrated that a high expression level of FBXL6 was indicative of poor prognosis in patients with glioma and was associated with decreased survival rates in these patients.

The expression of GCN5 has a considerable influence on glioma proliferation and invasion and is significantly associated with tumor grade (48,49). A previous study reported that GCN5 negatively regulated autophagy by inhibiting the biogenesis of autophagosomes and lysosomes, primarily through the targeting of transcription factor EB, a key autophagy and lysosome-related gene expression regulator (48). While the present study did not elucidate how the correlation between FBXL6 and GCN5 influenced glioma progression, future investigations are expected to provide a more comprehensive understanding of this relationship. A previous study reported that GCN5 can influence the progression of gliomas via the STAT3 and AKT pathways (48). As a histone acetyltransferase, GCN5 may work in conjunction with HMGA2 to facilitate the invasion and metastasis of glioma cells (50). The present study did not investigate the impact of epigenetics, thereby it is currently unclear whether FBXL6 impacts the epigenetic landscape in glioma cells. Nevertheless, future research should focus on epigenetic studies to investigate this further.

Nonetheless, these results collectively indicated the clinical value of FBXL6 as a potential prognostic biomarker for gliomas. The enrichment analysis conducted using GSEA demonstrated that FBXL6 was involved in various signaling pathways such as 'BUTANOATE_METABOLISM', 'CALCIUM_SIGNALING_PATHWAY', 'LONG_TERM_POTENTIATION', 'NOTCH_SIGNALING_PATHWAY' and 'PRIMARY_BILE_ACID_BIOSYNTHESIS'. These findings suggested that FBXL6 may affect the progression of glioma in patients through these pathways.

The role of FBXL6 in cell cycle regulation and tumorigenesis is important. However, current understanding of its prognostic value, underlying molecular mechanisms and drug sensitivity in gliomas remains incomplete. The present study confirmed that FBXL6 expression was significantly higher in gliomas compared with normal tissues, which suggested its potential impact on glioma malignancy. These findings highlighted FBXL6 as a candidate for a prognostic biomarker in glioma and as a potential target for neuroglioma treatment. Moreover, bioinformatics analysis demonstrated that FBXL6 may represent a viable future therapeutic target in glioma. Furthermore, IC₅₀ values indicated that drugs such as BMS345541, gefitinib, axitinib, bexarotene, foretinib, BHG712,

BX-795, BX-912 and phenformin exhibited enhanced efficacy in treating patients with glioma characterized by low FBXL6 expression levels.

Acknowledgements

Not applicable.

Funding

The present study was supported by research grants from the National Natural Science Foundation of China (grant no. 81830052) and the Shanghai Key Laboratory of Molecular Imaging (grant no. 18DZ2260400).

Availability of data and materials

The datasets generated in the present study may be requested from the corresponding author.

Authors' contributions

QL and SN guided the conception and design of the study. QL, JZ, WZ, HZ and ML collected clinical data and constructed figures. QL, JZ, HZ, SJ and JZ performed statistical analysis. JZ, SJ and SN revised the manuscript. QL and JZ conducted the second round of image acquisition and modifications. QL, JZ, WZ, HZ, ML, JZ, SJ and SN confirm the authenticity of all the raw data. All authors read and approved the final version of the manuscript.

Ethics approval and consent to participate

The study protocol was approved by the Ethics Committee of the Ninth People's Hospital, Shanghai Jiaotong University School of Medicine (approval no. H9H-2023-T489-1, Shanghai, China).

Patient consent for publication

Not applicable.

Competing interests

The authors declare that they have no competing interests.

References

- Ostrom QT, Bauchet L, Davis FG, Deltour I, Fisher JL, Langer CE, Pekmezci M, Schwartzbaum JA, Turner MC, Walsh KM, *et al.*: The epidemiology of glioma in adults: A 'state of the science' review. *Neuro Oncol* 16: 896-913, 2014.
- Molinaro AM, Taylor JW, Wiencke JK and Wrensch MR: Genetic and molecular epidemiology of adult diffuse glioma. *Nat Rev Neurol* 15: 405-417, 2019.
- Cancer Genome Atlas Research Network; Brat DJ, Verhaak RG, Aldape KD, Yung WK, Salama SR, Cooper LA, Rheinbay E, Miller CR, Vitucci M, *et al.*: Comprehensive, integrative genomic analysis of diffuse lower-grade gliomas. *N Engl J Med* 372: 2481-2498, 2015.
- Louis DN, Ohgaki H, Wiestler OD, Cavenee WK, Burger PC, Jouvet A, Scheithauer BW and Kleihues P: The 2007 WHO classification of tumours of the central nervous system. *Acta Neuropathol* 114: 97-109, 2007.

5. Yuan B, Wang G, Tang X, Tong A and Zhou L: Immunotherapy of glioblastoma: Recent advances and future prospects. *Hum Vaccin Immunother* 18: 2055417, 2022.
6. Stupp R, Mason WP, van den Bent MJ, Weller M, Fisher B, Taphoorn MJ, Belanger K, Brandes AA, Marosi C, Bogdahn U, *et al*: Radiotherapy plus concomitant and adjuvant temozolomide for glioblastoma. *N Engl J Med* 352: 987-996, 2005.
7. Roukens MG, Alloul-Ramdhani M, Moghadasi S, Op den Brouw M and Baker DA: Downregulation of vertebrate Tel (ETV6) and Drosophila Yan is facilitated by an evolutionarily conserved mechanism of F-box-mediated ubiquitination. *Mol Cell Biol* 28: 4394-4406, 2008.
8. Bonacci T and Emanuele MJ: Dissenting degradation: Deubiquitinases in cell cycle and cancer. *Semin Cancer Biol* 67: 145-158, 2020.
9. Abbas R and Larisch S: Killing by degradation: Regulation of apoptosis by the ubiquitin-proteasome-system. *Cells* 10: 3465, 2021.
10. Daulny A and Tansey WP: Damage control: DNA repair, transcription, and the ubiquitin-proteasome system. *DNA Repair (Amst)* 8: 444-448, 2009.
11. Bendotti C, Marino M, Cheroni C, Fontana E, Crippa V, Poletti A and De Biasi S: Dysfunction of constitutive and inducible ubiquitin-proteasome system in amyotrophic lateral sclerosis: Implication for protein aggregation and immune response. *Prog Neurobiol* 97: 101-126, 2012.
12. Han D, Wang L, Jiang S and Yang Q: The ubiquitin-proteasome system in breast cancer. *Trends Mol Med* 29: 599-621, 2023.
13. Reinstein E and Ciechanover A: Narrative review: Protein degradation and human diseases: The ubiquitin connection. *Ann Intern Med* 145: 676-684, 2006.
14. Dang F, Nie L and Wei W: Ubiquitin signaling in cell cycle control and tumorigenesis. *Cell Death Differ* 28: 427-438, 2021.
15. Ciechanover A: The unravelling of the ubiquitin system. *Nat Rev Mol Cell Biol* 16: 322-324, 2015.
16. Chan CH, Li CF, Yang WL, Gao Y, Lee SW, Feng Z, Huang HY, Tsai KK, Flores LG, Shao Y, *et al*: The Skp2-SCF E3 ligase regulates Akt ubiquitination, glycolysis, herceptin sensitivity, and tumorigenesis. *Cell* 149: 1098-1111, 2012.
17. Meng X, Liu X, Guo X, Jiang S, Chen T, Hu Z, Liu H, Bai Y, Xue M, Hu R, *et al*: FBXO38 mediates PD-1 ubiquitination and regulates anti-tumour immunity of T cells. *Nature* 564: 130-135, 2018.
18. Wang Z, Liu P, Inuzuka H and Wei W: Roles of F-box proteins in cancer. *Nat Rev Cancer* 14: 233-247, 2014.
19. Wu J, Zhang X, Zhang L, Wu CY, Rezaeian AH, Chan CH, Li JM, Wang J, Gao Y, Han F, *et al*: Skp2 E3 ligase integrates ATM activation and homologous recombination repair by ubiquitinating NBS1. *Mol Cell* 46: 351-361, 2012.
20. Nelson DE, Randle SJ and Laman H: Beyond ubiquitination: The atypical functions of Fbxo7 and other F-box proteins. *Open Biol* 3: 130131, 2013.
21. Chen D, Liu X, Xia T, Tekcham DS, Wang W, Chen H, Li T, Lu C, Ning Z, Liu X, *et al*: A multidimensional characterization of E3 ubiquitin ligase and substrate interaction network. *iScience* 16: 177-191, 2019.
22. Li Y, Cui K, Zhang Q, Li X, Lin X, Tang Y, Prochownik EV and Li Y: FBXL6 degrades phosphorylated p53 to promote tumor growth. *Cell Death Differ* 28: 2112-2125, 2021.
23. Yu Y, Yao W, Wang T, Xue W, Meng Y, Cai L, Jian W, Yu Y and Zhang C: FBXL6 depletion restrains clear cell renal cell carcinoma progression. *Transl Oncol* 26: 101550, 2022.
24. Shi W, Feng L, Dong S, Ning Z, Hua Y, Liu L, Chen Z and Meng Z: FBXL6 governs c-MYC to promote hepatocellular carcinoma through ubiquitination and stabilization of HSP90AA1. *Cell Commun Signal* 18: 100, 2020.
25. Schiff D: Low-grade gliomas. *Continuum (Minneapolis)* 23: 1564-1579, 2017.
26. Russell B, Collins A, Dally M, Dowling A, Gold M, Murphy M and Philip J: Living longer with adult high-grade glioma: Setting a research agenda for patients and their caregivers. *J Neurooncol* 120: 1-10, 2014.
27. Ding H, Zhao J, Zhang Y, Yu J, Liu M, Li X, Xu L, Lin M, Liu C, He Z, *et al*: Systematic analysis of drug vulnerabilities conferred by tumor suppressor loss. *Cell Rep* 27: 3331-3344.e6, 2019.
28. Dai Z, Wu J, Chen F, Cheng Q, Zhang M, Wang Y, Guo Y and Song T: CXCL5 promotes the proliferation and migration of glioma cells in autocrine- and paracrine-dependent manners. *Oncol Rep* 36: 3303-3310, 2016.
29. Livak KJ and Schmittgen TD: Analysis of relative gene expression data using real-time quantitative PCR and the 2(-Delta Delta C(T)) method. *Methods* 25: 402-408, 2001.
30. Zhang J, Lin XT, Yu HQ, Fang L, Wu D, Luo YD, Zhang YJ and Xie CM: Elevated FBXL6 expression in hepatocytes activates VRK2-transketolase-ROS-mTOR-mediated immune evasion and liver cancer metastasis in mice. *Exp Mol Med* 55: 2162-2176, 2023.
31. Wu W, Klockow JL, Zhang M, Lafortune F, Chang E, Jin L, Wu Y and Daldrop-Link HE: Glioblastoma multiforme (GBM): An overview of current therapies and mechanisms of resistance. *Pharmacol Res* 171: 105780, 2021.
32. Chinot OL, Wick W, Mason W, Henriksson R, Saran F, Nishikawa R, Carpentier AF, Hoang-Xuan K, Kavan P, Cernea D, *et al*: Bevacizumab plus radiotherapy-temozolomide for newly diagnosed glioblastoma. *N Engl J Med* 370: 709-722, 2014.
33. Chen J, McKay RM and Parada LF: Malignant glioma: Lessons from genomics, mouse models, and stem cells. *Cell* 149: 36-47, 2012.
34. Liu LY, Ji MS, Nguyen NT, Chow FE, Molaie DM, Pianka ST, Green RM, Liau LM, Ellingson BM, Nghiemphu PL, *et al*: Patterns of long-term survivorship following bevacizumab treatment for recurrent glioma: A case series. *CNS Oncol* 8: CNS35, 2019.
35. Ghorbani A, Avery LM, Sohaei D, Soosaipillai A, Richer M, Horbinski C, McCortney K, Xu W, Diamandis EP and Prassas I: Discovery of novel glioma serum biomarkers by proximity extension assay. *Clin Proteomics* 20: 12, 2023.
36. Cheng J, Guo J, Wang Z, North BJ, Tao K, Dai X and Wei W: Functional analysis of Cullin 3 E3 ligases in tumorigenesis. *Biochim Biophys Acta Rev Cancer* 1869: 11-28, 2018.
37. Naseem Y, Zhang C, Zhou X, Dong J, Xie J, Zhang H, Agboyibor C, Bi Y and Liu H: Inhibitors targeting the F-BOX proteins. *Cell Biochem Biophys* 81: 577-597, 2023.
38. D'Angiolella V, Donato V, Vijayakumar S, Saraf A, Florens L, Washburn MP, Dynlacht B and Pagano M: SCF(Cyclin F) controls centrosome homeostasis and mitotic fidelity through CP110 degradation. *Nature* 466: 138-142, 2010.
39. Rye MS, Wiertsema SP, Scaman ES, Oommen J, Sun W, Francis RW, Ang W, Pennell CE, Burgner D, Richmond P, *et al*: FBXO11, a regulator of the TGFβ pathway, is associated with severe otitis media in Western Australian children. *Genes Immun* 12: 352-359, 2011.
40. Duan S, Cermak L, Pagan JK, Rossi M, Martinengo C, di Celle PF, Chapuy B, Shipp M, Chiarle R and Pagano M: FBXO11 targets BCL6 for degradation and is inactivated in diffuse large B-cell lymphomas. *Nature* 481: 90-93, 2012.
41. Santra MK, Wajapeyee N and Green MR: F-box protein FBXO31 mediates cyclin D1 degradation to induce G1 arrest after DNA damage. *Nature* 459: 722-725, 2009.
42. Yoshida Y, Tokunaga F, Chiba T, Iwai K, Tanaka K and Tai T: Fbs2 is a new member of the E3 ubiquitin ligase family that recognizes sugar chains. *J Biol Chem* 278: 43877-43884, 2003.
43. Yoshida Y, Chiba T, Tokunaga F, Kawasaki H, Iwai K, Suzuki T, Ito Y, Matsuoka K, Yoshida M, Tanaka K and Tai T: E3 ubiquitin ligase that recognizes sugar chains. *Nature* 418: 438-442, 2002.
44. Frescas D and Pagano M: Deregulated proteolysis by the F-box proteins SKP2 and beta-TrCP: Tipping the scales of cancer. *Nat Rev Cancer* 8: 438-449, 2008.
45. Nakayama KI and Nakayama K: Regulation of the cell cycle by SCF-type ubiquitin ligases. *Semin Cell Dev Biol* 16: 323-333, 2005.
46. Maser RS, Choudhury B, Campbell PJ, Feng B, Wong KK, Protopopov A, O'Neil J, Gutierrez A, Ivanova E, Perna I, *et al*: Chromosomally unstable mouse tumours have genomic alterations similar to diverse human cancers. *Nature* 447: 966-971, 2007.
47. Menyhart O and Györfy B: Multi-omics approaches in cancer research with applications in tumor subtyping, prognosis, and diagnosis. *Comput Struct Biotechnol J* 19: 949-960, 2021.
48. Liu K, Zhang Q, Lan H, Wang L, Mou P, Shao W, Liu D, Yang W, Lin Z, Lin Q and Ji T: GCN5 Potentiates glioma proliferation and invasion via STAT3 and AKT signaling pathways. *Int J Mol Sci* 16: 21897-21910, 2015.
49. Ouyang C, Mu J, Lu Q, Li J, Zhu H, Wang Q, Zou MH and Xie Z: Autophagic degradation of KAT2A/GCN5 promotes directional migration of vascular smooth muscle cells by reducing TUBA/α-tubulin acetylation. *Autophagy* 16: 1753-1770, 2020.
50. Zhang S, Zhang H and Yu L: HMGA2 promotes glioma invasion and poor prognosis via a long-range chromatin interaction. *Cancer Med* 7: 3226-3239, 2018.

